The potential to breed for genetic legacy effects in sustainable farming systems

Shanice Van Haeften[1#], Stephanie M. Brunner[1#], Eric Dinglasan[1], Edward Fabreag[1], Joseph Eyre[1], Celine Mens[1], Ben J Hayes[1], Michael Udvardi[1], Samir Alahmad[1], Mitchell Eglinton[1], Ryan McQuinn[2], Merrill Ryan[3], Sarah van der Meer[1], Millicent R. Smith[1,4]*, Lee T. Hickey[1*]

[1]Queensland Alliance for Agriculture and Food Innovation, The University of Queensland, QLD, Australia

[2]School of Science, Western Sydney University, NSW, Australia

[3]Queensland Department of Primary Industries, Warwick, QLD, Australia

[4]School of Agriculture and Food Sustainability, Faculty of Science, The University of Queensland, QLD, Australia

[#]Shanice Van Haeften and Stephanie M. Brunner contributed equally to this work.

Correspondence: Lee T. Hickey and Millicent R. Smith are co-corresponding authors.

Email: l.hickey@uq.edu.au

Email: millicent.smith@uq.edu.au

Abstract

Legume crops provide protein-rich food, critical disease breaks in cereal rotations, and contribute to soil fertility through symbiotic nitrogen fixation. However, crop improvement programs typically focus on individual crop performance rather than system-level benefits. We hypothesise that legacy effects (the influence of one crop's genotype on subsequent crop performance) are under genetic control and could be leveraged in breeding programs. To test this, we evaluated how 309 genetically diverse mungbean genotypes influence subsequent wheat performance. The mungbean panel was grown, followed by a single wheat cultivar sown in the same plot locations. Remarkably, wheat yield varied by nearly 1 t ha^{-1} (2.52-3.49 t ha^{-1}) depending solely on the preceding mungbean genotype, with legacy traits displaying moderate heritability (H^2: 0.43-0.65), demonstrating untapped genetic potential for breeding. Integrated analyses of traits, soil properties, and volatile organic compounds identified potential biological drivers including root architecture, symbiotic nitrogen fixation and soil microbiome. Haplotype mapping identified genomic regions in mungbean associated with wheat yield and protein, revealing trade-offs between direct and legacy performance. Genetic simulations using empirically derived marker effects compared genomic selection strategies targeting mungbean yield, wheat yield, or both simultaneously. Balanced selection (50:50 weighting) achieved simultaneous gains in both crops (19.5% and 7.6%), highlighting the opportunity to breed for system-level productivity with reduced input requirements.

Introduction

Modern crop breeding programs typically aim to optimise a single species, focusing on traits that enhance yield and quality, irrespective of the preceding or subsequent crops in rotation (Bennett et al., 2012). This approach achieved remarkable success during the Green Revolution, transforming wheat and rice production through high-yielding cultivars that fed billions globally, though often requiring increased fertiliser and irrigation inputs (Evenson and Gollin, 2003). Importantly, breeding remains effective even in low-input systems, as demonstrated by continued genetic gains across diverse production environments (Voss-Fels et al., 2019). However, the global population will approach 10 billion by 2050, and agricultural systems have become increasingly reliant on external inputs. Nitrogen fertiliser use has increased over 40% globally since 1990 (Li et al., 2025) and is projected to increase further to meet growing food demand, despite environmental and climate concerns. This calls for innovative breeding strategies to accelerate the development of more productive and

sustainable crops (Hickey et al., 2019), particularly as the single-crop breeding paradigm may be missing critical genetic opportunities when the farming system is holistically considered.

Emerging evidence suggests that genetic variation within crop species creates measurable effects on subsequent crops in rotation (Rose et al., 2010; Ellouze et al., 2013), yet the genetic basis of these "legacy effects" remains largely unexplored. Legacy effects occur when the genetic characteristics of one crop influence the performance of subsequent crops through persistent changes to soil conditions that carry over between growing seasons (Somenahally et al., 2018; Lilley and Kirkegaard, 2016). While the benefits of crop rotations at the cross-species level are well established, for example legumes fixing nitrogen for cereals (e.g. Zhao et al., 2022), crop rotations to break disease cycles (e.g. Kirkegaard et al., 1997), and diverse root systems improving soil structure (e.g. Yu et al., 2025), the genetic variation within species that could enhance these rotational benefits through targeted breeding remains untapped in current breeding programs. Lilley and Kirkegaard (2016) highlight this concept, demonstrating that wheat cultivars with deeper, more extensive root systems extracted additional subsoil water but left soils drier at subsequent crop sowing, reducing predicted yield benefits when legacy effects were considered. Thus, selection for deeper root architecture within wheat breeding germplasm could lead to higher yielding wheat cultivars, but they may result in unintended negative consequences for subsequent crops. Integrating legumes into crop rotations enriches soil nitrogen through symbiotic nitrogen fixation, benefiting subsequent crops with yield increases often exceeding 10% and with substantial reductions in fertiliser requirements (Cernay et al., 2018; Zhao et al., 2022). However, the extent to which genetic variation within legume crop species modulates both positive and negative legacy effects remains unexplored.

We hypothesise that the genetic architecture of a crop can directly modulate the performance of the subsequent crop, creating legacy effects that can be leveraged through breeding to optimise integrated farming system productivity (Fig 1). To test this, we conducted a proof-of-concept study using mungbean (*Vigna radiata*) as a preceding legume crop in a wheat-based rotation system. Mungbean contributes to the system by fixing nitrogen and providing a disease break, thereby enhancing the productivity and health of the subsequent wheat crop (Ilyas et al., 2018; Foyer, Nguyen & Lam, 2019). We evaluated how 309 genetically diverse mungbean accessions influenced performance of a subsequent wheat crop rotation, combined with haplotype mapping to identify genomic regions influencing both direct mungbean traits and legacy effects on wheat productivity and quality. Through genetic simulations using real haplotype effects, we further evaluated the potential of breeding programs that systematically

consider legacy traits alongside traditional performance metrics. These simulations were used to determine whether such integrated approaches could improve genetic gain and productivity for both crops through enhanced resource-use efficiency.

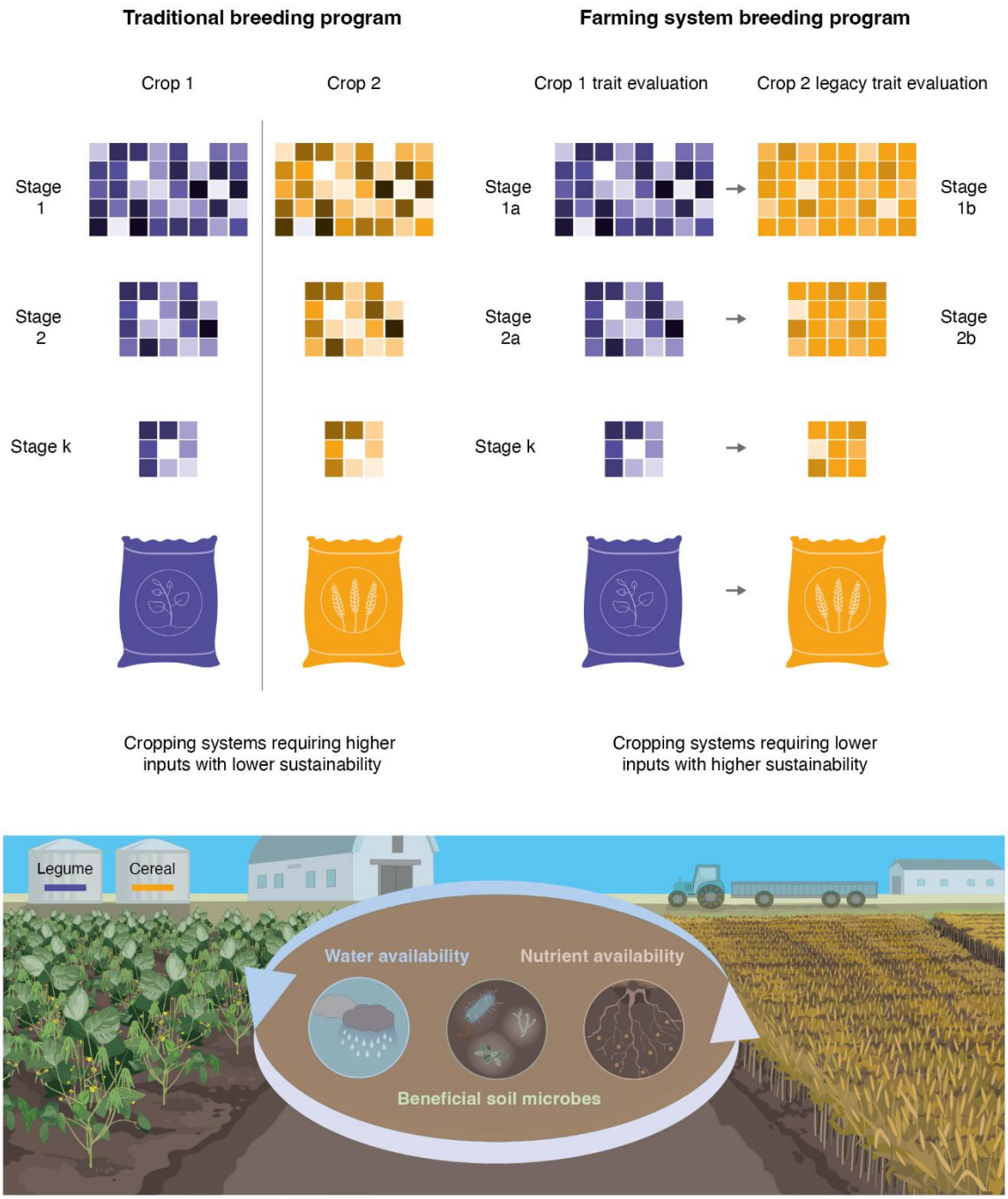

Fig 1. Conceptual framework for integrating legacy traits into farming systems breeding. *Comparison of traditional breeding (optimising crop performance in isolation) with farming systems breeding that considers genetic effect of one crop on the next (legacy traits) within rotational systems. In the farming systems approach, Crop 1 is evaluated for both direct*

performance traits and legacy effects on Crop 2 (Stage 1a), followed by assessment of Crop 2's legacy trait expression (Stage 1b), with dual evaluation continuing through subsequent breeding stages. The lower panel illustrates how considering legacy traits could enable selection of genotypes that enhance system productivity through improved water-use efficiency, nutrient-use efficiency, and beneficial soil properties, including microbiome. This framework represents a potential paradigm shift toward multi-crop, multi-season breeding supporting sustainable intensification with reduced input requirements.

Results

High and heritable legacy trait variation across mungbean genotypes

In the mungbean mini-core panel, substantial phenotypic variation with moderate broad-sense heritability was observed across all measured mungbean traits (Fig. 2a; Supplementary Tables 1 and 2). Mungbean yield varied 11-fold from 0.21 to 2.19 t ha^{-1}, with the check cultivar Crystal producing 1.31 t ha^{-1}. Mungbean aboveground biomass at mid canopy development showed 2.6-fold variation (151.1 to 393.3 g m^{-2}; Crystal 280.7 g m^{-2}). Vegetation index values derived from UAV-based imaging (mungbean NDRE) at 90% black pod exhibited 2.5-fold variation (0.18 to 0.45; Crystal: 0.23), indicating considerable genotypic diversity in canopy vigour and greenness. All mungbean traits exhibited high heritability (H^2 = 0.63–0.84).

To quantify legacy effects after harvest of the mungbean genotypes, we measured wheat yield for the single cultivar LongReach Raider. Wheat yield varied substantially by preceding mungbean genotype (2.52 to 3.49 t ha^{-1}; Crystal 3.06 t ha^{-1}). Wheat protein content varied from 7.36% to 8.48% (Crystal: 8.14%), while wheat NDRE ranged from 0.38 to 0.43 (Crystal: 0.41). Critically, wheat legacy traits showed moderate heritability (H^2 = 0.43–0.65), indicating that a substantial portion of variation in wheat performance was attributable to mungbean genotype. Individual mungbean genotypes enhanced subsequent wheat yield by up to 45% or reduced it by as much as 50% relative to Crystal, underscoring the major impact of mungbean genotype on rotational crop productivity (Fig. 2b).

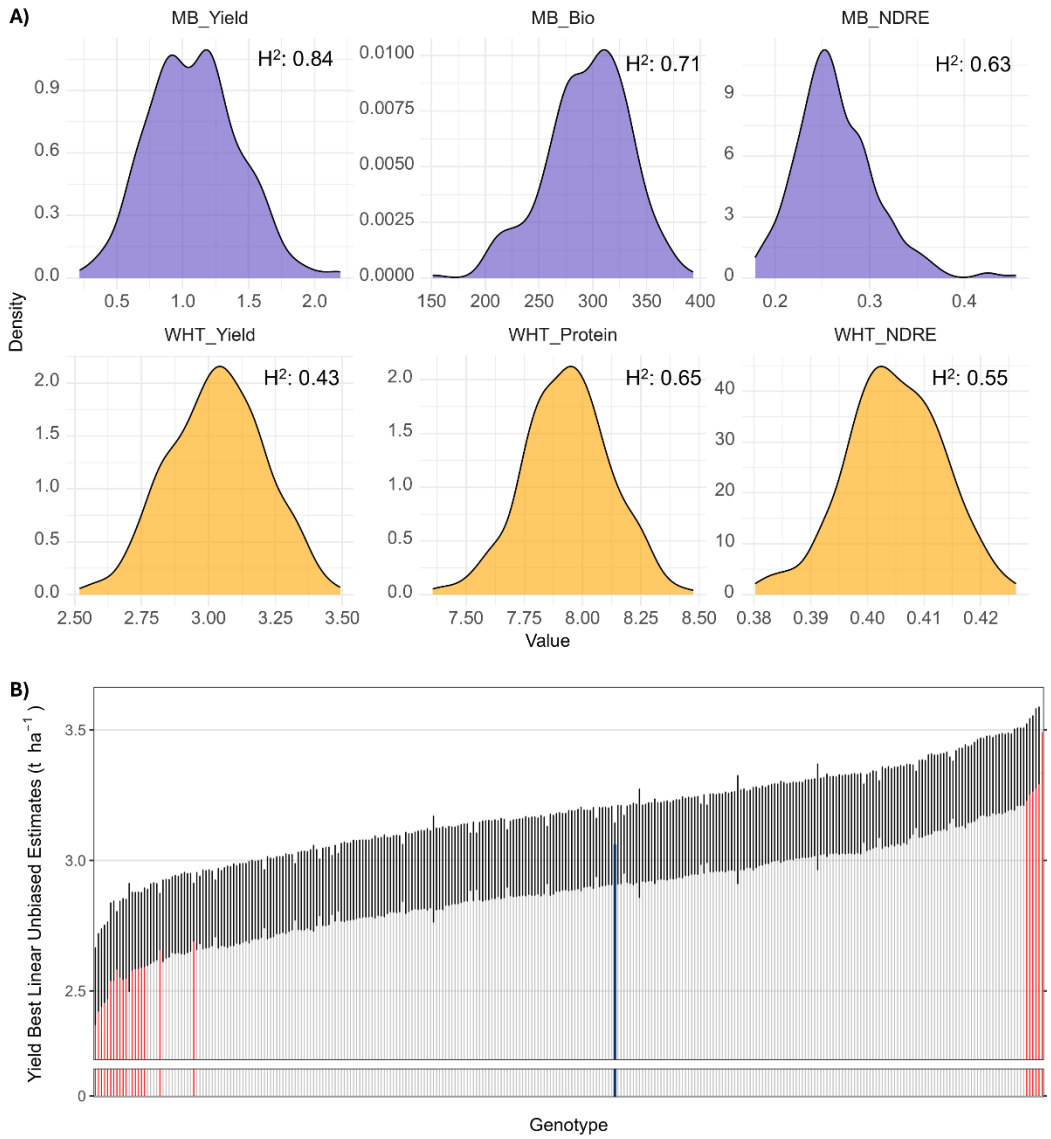

Fig 2. Genotypic variation and heritability of mungbean traits and wheat legacy effects. *a) Distribution of phenotypic values for direct mungbean traits (yield, biomass, NDRE; purple) and wheat legacy traits (yield, grain protein, NDRE; orange) across 309 genotypes. Broad-sense heritability (H^2) for each trait is displayed in the top-right corner. b) Wheat yield performance ordered by increasing yield (t ha^{-1}), reflecting legacy effects from preceding mungbean genotypes. Each bar represents the BLUE ± standard error for wheat following an individual mungbean genotype. Blue bar indicates wheat following the check cultivar 'Crystal'; red bars indicate wheat yields significantly different from 'Crystal' ($p < 0.05$).*

Interactions between direct and legacy traits reveal trade-offs

Relationships between mungbean and wheat legacy traits varied in directionality and strength when evaluated across phenotypic, genetic, and haplotype levels (Fig. 3). At the phenotypic level (Fig 3a), mungbean yield showed a moderate negative correlation with wheat yield ($r = -0.39$, $p < 0.05$), suggesting potential trade-offs between mungbean productivity and subsequent crop performance. In contrast, wheat NDRE measured at flowering and wheat yield were positively correlated ($r = 0.75$, $p < 0.05$), indicating consistency among wheat physiological performance metrics. Wheat NDRE at flowering also showed a significant negative correlation with mungbean yield ($r = -0.48$, $p < 0.05$).

Genetic correlations revealed stronger associations, highlighting underlying genetic relationships not evident at the phenotypic level (Fig 3b). Mungbean NDRE at 90% black pod exhibited strong negative genetic correlations with all wheat traits (wheat yield $r = -0.90$; wheat protein $r = -0.95$; wheat NDRE $r = -0.92$), suggesting that genetic architecture underlying mungbean canopy greeness and health indicators captured by NDRE late in the season may be antagonistic to wheat legacy performance. In contrast, mungbean yield showed moderately low negative genetic correlation with mungbean biomass ($r = -0.32$) and wheat yield ($r = -0.29$), but a strong positive genetic correlation with wheat protein ($r = 0.73$). Wheat protein displayed positive genetic relationships with wheat NDRE at flowering ($r = 0.68$), wheat biomass ($r = 0.88$) and wheat yield ($r = 0.67$), as well as with mungbean biomass ($r = 0.88$) reinforcing coherence among performance traits within and across species.

Haplotype-level variance correlations were uniformly positive across all mungbean and wheat traits ($r = 0.28$–0.78, $p < 0.05$), indicating that shared genomic regions contribute to trait variation across the mungbean–wheat system (Fig 3c). However, haplotype effect correlations revealed more nuanced patterns, including directional shifts between traits (Fig 3d). Mungbean yield showed strong negative haplotype effect correlations with wheat yield ($r = -0.61$, $p < 0.05$) and wheat NDRE ($r = -0.77$, $p < 0.05$), but positive associations with mungbean biomass ($r = 0.60$, $p < 0.05$) and wheat protein ($r = 0.70$, $p < 0.05$). These contrasting directions suggest trade-offs at the genome level and highlight key haplotypes that differentially influence mungbean performance and legacy benefits to wheat.

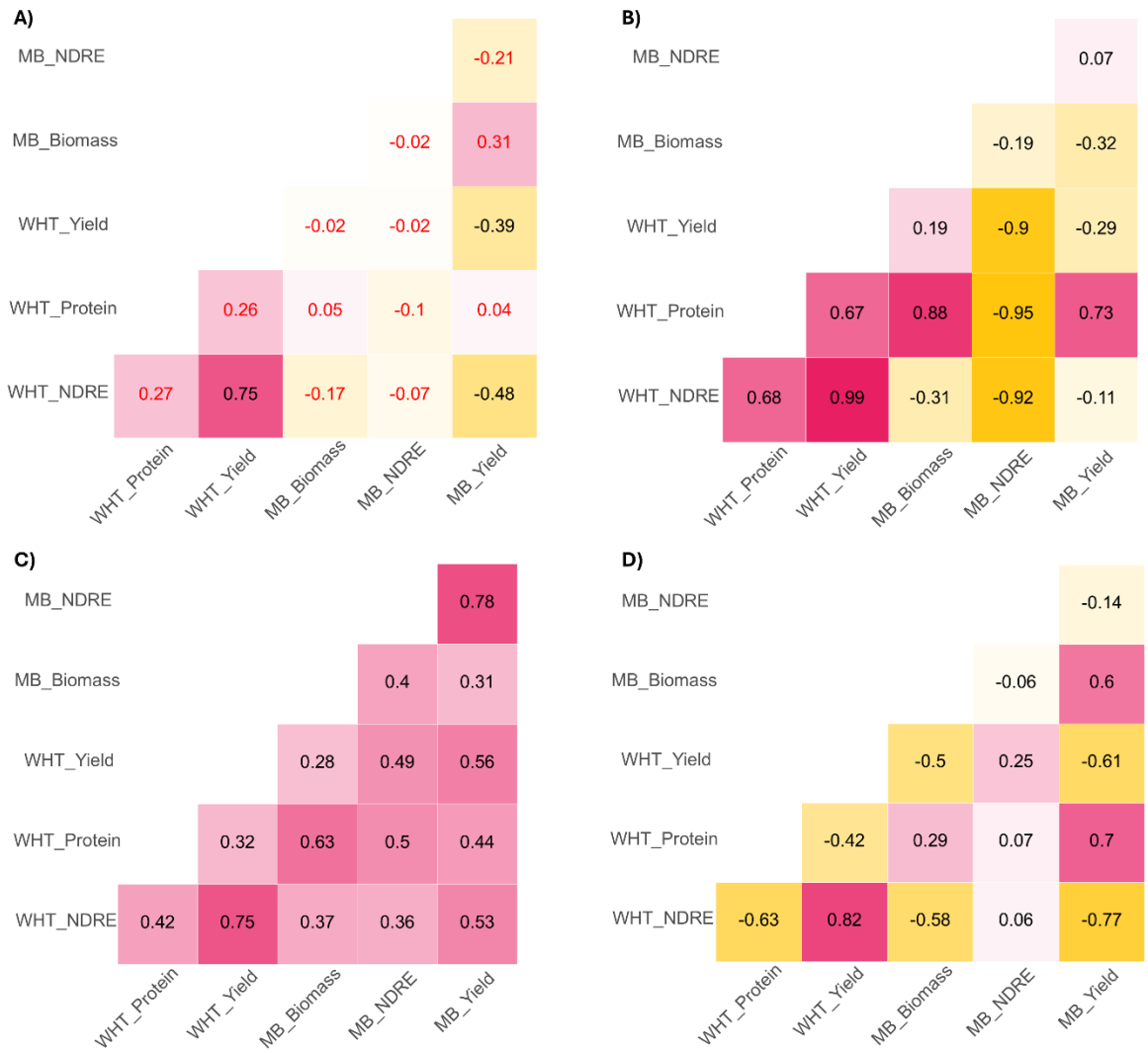

Fig 3. Correlations among mungbean and wheat legacy traits at phenotypic, genetic, and haplotype levels. *A) Phenotypic correlations (r) based on BLUEs across all genotypes. B) Genetic correlations estimated from mixed-model variance components, indicating shared genetic architecture between traits. C) Haplotype-level variance correlations, indicating shared genomic regions contributing to trait variation. D) Haplotype effect correlations, quantifying concordance in direction and magnitude of haplotype influences across traits. Colour scale ranges from 1 (pink, positive correlation) through -1 (yellow, negative correlation). Non-significant correlations ($p > 0.05$) are indicated in red text.*

We selected the top 12 haploblocks with highest variance for each trait, identifying 33 unique haploblocks across all traits (Supplementary Table 3). Seventeen haploblocks were unique to single traits, with eight showing high variance for wheat legacy effects but not for any measured mungbean traits (Fig 4a and Supplementary Fig 1). The remaining 16 haploblocks showed high

variance for at least two traits across both wheat and mungbean. One haploblock (b000055, chr 1) showed high variance for all six traits across both species. Three additional haploblocks, b000160 (chr 2), b000221 (chr 3), and b000509 (chr 5), showed high variance for five of six traits, suggesting that these genomic regions harbour loci with pleiotropic effects within mungbean, and genetically mediated legacy effects influencing wheat traits in rotation systems.

Among the top haploblocks, five were shared between mungbean yield and wheat yield (Fig. 4a): b000022 (chr 1), b000055 (chr 1), b000221 (chr 2), b000253 (chr 2), and b000509 (chr 5), while seven high-variance haploblocks did not overlap between crops. This pattern indicates both shared and independent genetic control of direct versus legacy traits.

Functional genes associated with nitrogen fixation in legumes were positioned within five top haploblocks identified in this study (Supplementary Table 4). Co-located genes were associated with broader root development processes, including gibberellin signalling (*MtDELLA2*), root meristem maintenance (*MtPLT1–4*), and auxin transport (*MtPIN2–4*), suggesting that root architecture may be a key mechanism underlying legacy effects.

To dissect these relationships at higher resolution, we examined two haploblocks in detail: b000055 (chr 1), the only haploblock with high variance for all six traits, and b000942 (chr 10), a haploblock with high variance for wheat yield but not ranking among the top 12 for mungbean yield. At haploblock b000055, haplotypes with the strongest positive effects for mungbean yield were associated with greater negative effects on wheat yield, consistent with the overall negative genetic correlation (Fig. 4b). This pattern illustrates the genomic basis of trade-offs between direct crop performance and legacy benefits. In contrast, block b000942 was not among the highest-variance regions for mungbean yield but nonetheless exhibited haplotype variance comparable to that observed for wheat, where it ranked among the top variance haploblocks. This haploblock harboured haplotypes with positive effects for both mungbean and wheat yield, as well as variants with neutral effects, indicating opportunities to select haplotypes beneficial for system-wide productivity without compromising individual crop performance.

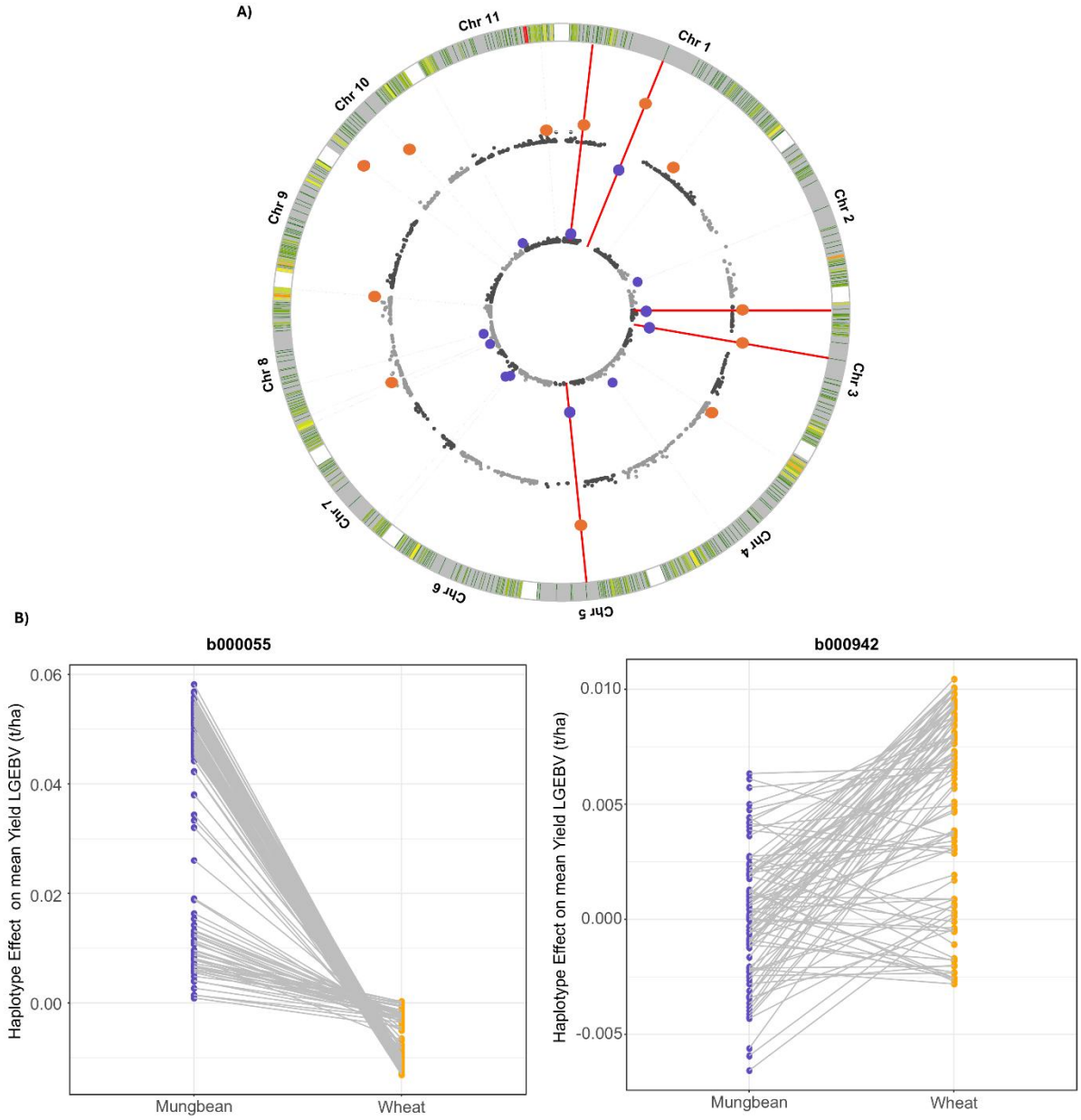

194

195 ***Figure 4. Haploblocks associated with mungbean yield and legacy effects on wheat yield.***
196 *a) Circos plot displaying haploblock effect variance for yield in mungbean (inner ring) and*
197 *wheat (outer ring) across the 11 mungbean chromosomes. The top 1% of haploblocks by*
198 *variance are highlighted for each crop (mungbean purple, wheat orange). Red lines connect*
199 *shared high variance haploblocks between crops, indicating loci with pleiotropic effects on*
200 *system-level productivity. b) Haplotype effects for mungbean and wheat yield at two*
201 *representative haploblocks: b000055 (chr 1) showing trade-offs, and b000942 (chr 10)*
202 *showing aligned effects across both species.*

Simulated selection strategies reveal challenges and opportunities for system-level yield optimisation

To evaluate the potential for simultaneous genetic improvement of mungbean and its legacy effects on wheat, we simulated genomic selection strategies using variable weighting schemes for the two crops over 25 breeding cycles, using the real haplotype effects as a starting point. Simulated progenies were generated by sampling chromosomes with recombination from selected parents (e.g. Villiers et al., 2022). When haplotypes were selected solely to maximise mungbean yield (100% mungbean weighting), predicted genomic estimated breeding values for mungbean increased by 36.86% over the 25 cycles. However, this improvement came at a cost to the subsequent crop, with legacy wheat yield showing a 7.71% reduction, highlighting the presence of antagonistic haplotypes that benefit mungbean but negatively impact wheat performance.

Adjusting the selection index to include moderate wheat emphasis (70:30 mungbean:wheat weighting) maintained high genetic gain in mungbean (36.32%) while moderating the negative legacy impact on wheat (reduced to 4.59% loss), demonstrating a more balanced trade-off between direct and legacy benefits. In contrast, placing greater emphasis on wheat legacy performance (30:70 weighting) yielded strong improvements in wheat legacy yield (13.44% increase) with a modest decline in mungbean yield (22.56% reduction), indicating that prioritising legacy traits can substantially benefit the subsequent crop, albeit at a considerable cost to the initial crop.

Selection based on equal weighting (50:50) resulted in simultaneous yield gains for both mungbean and wheat (19.45% and 7.55%, respectively), though the overall magnitude of improvement was lower than in crop-specific optimisation scenarios. This balanced approach demonstrates the potential of system-wide genetic improvement through integrated breeding strategies that consider both direct performance and legacy effects. The simulation results reveal that while trade-offs exist between optimising individual crop performance versus rotational benefits, strategic selection can achieve meaningful gains across the entire cropping system, providing a pathway for sustainable intensification through breeding.

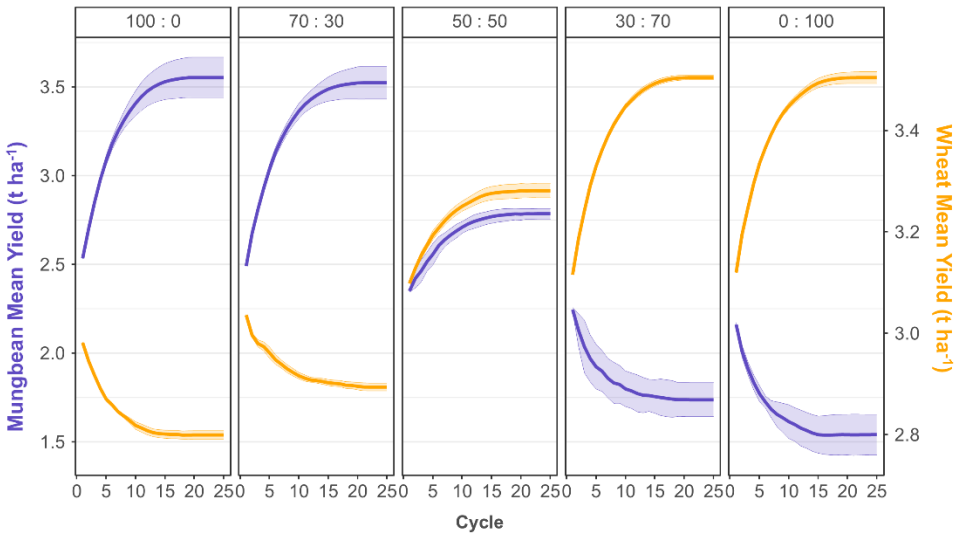

Fig 5. Simulated selection strategies reveal trade-offs and optimisation potential for breeding mungbean with system-level benefits. *Genomic estimated breeding values (GEBVs) for mungbean yield (purple) and wheat legacy yield (orange) over 25 breeding cycles under five selection strategies. From left to right: 100% mungbean yield, 70:30 mungbean:wheat, 50:50 equal weighting, 30:70 mungbean:wheat, and 100% wheat legacy yield. Lines show mean GEBVs with 95% confidence intervals (shaded regions).*

Analysis of soil properties reveals genetic variation for biological drivers of legacy effects

To explore potential traits contributing to legacy effects on subsequent crops, we sampled and analysed soil from a subset of 10 genetically diverse mungbean genotypes after mungbean harvest and prior to wheat sowing. Among the soil nutrient parameters assessed, nitrate (NO_3^-) levels differed significantly between genotypes (p = 0.01), indicating genotype-dependent variation in soil nitrogen dynamics. In contrast, no significant genotypic differences were detected for other soil nutrient components, including ammonium, phosphorus, or exchangeable cations (Supplementary Table 5).

To investigate possible differences in soil microbiome associated with mungbean genotype, we analysed soil volatile organic compounds (VOCs) for the same subset (Supplementary Table 6). Out of 143 VOCs detected in soil samples, 25 passed quality filter criteria, of which eleven showed significant genotypic effects (Supplementary Fig. 2). Dehydrocamphor and 2-methylisoborneol displayed the largest genotypic differences, with cultivar Crystal showing elevated abundance compared to bare soil control and other genotypes (Supplementary Fig. 3 and Supplementary Table 7). Berken displayed a distinct VOC profile with elevated levels of

multiple compounds including 1,4-cis-dimethylcyclooctane, 4,5-dimethylnonane, and 3,7-dimethyloctan-1-ol compared to other genotypes and bare soil. Several mungbean genotypes were associated with significantly reduced accumulation of specific VOCs (3-methoxy-3-methylbutanol and styrene) compared to bare soil (Supplementary Fig. 3 and Supplementary Table 7), indicating potential for genotypic regulation of soil microbiome diversity.

Discussion

While agricultural research has long demonstrated the value of crop rotations, this study reveals for the first time the potential for rotational benefits to be enhanced through targeted plant breeding by selecting genotypes that shape the environment in ways that influence the performance of subsequent crops. To date, research has focused on species-level benefits (e.g., Li et al., 2019; Lago-Olveira et al., 2023; Salvagiotti et al., 2024), such as nitrogen fixation or disease suppression, rather than legacy variation between genotypes within the initial crop. Our results show that crop legacy effects are under genetic control.

In our mungbean-wheat rotation system, substantial phenotypic variation in wheat NDRE, yield and protein content was observed as a function of the preceding mungbean genotype. Importantly, these legacy traits exhibited moderate heritability ($H^2 = 0.43–0.65$), demonstrating that they are amenable to selection. Remarkably, mungbean genotypes enhanced subsequent wheat yield by up to 45% or reduced it by 50% relative to the commercial check variety, revealing substantial genetic variation in legacy effects beyond environmental variation alone. These results highlight a real limitation in traditional breeding that focuses on maximising the performance of a single crop, making an implicit assumption that any effect on subsequent crops is negligible. In contrast, our results demonstrate that legacy effects vary across genotypes and can have a substantial effect on following crops. This reveals an opportunity for a fundamental shift in breeding philosophy, from exploiting fixed species-level rotational benefits to harnessing genetic variation within species for enhanced system-wide productivity.

Another novel concept demonstrated in this study is that legacy effects can be genetically mapped to the genome of the prior rotation crop. The legacy traits investigated in this case study exhibited complex genetic architecture, with many agronomic traits showing shared genetic control. We identified both shared and unique haploblocks influencing direct mungbean traits and legacy effects on wheat, with 16 high-variance haploblocks showing overlapping effects across both crops. The magnitude of haplotype effects was consistently greater for mungbean traits than for legacy impacts on wheat. This is somewhat expected, as there are

285 many other factors contributing to wheat performance beyond legacy effects, including the
286 underlying genetics of the wheat cultivar and seasonal growing conditions. Several top
287 haploblocks contained functional genes associated with root development processes, including
288 gibberellin signalling (*MtDELLA2*), root meristem maintenance (*MtPLT1–4*), and auxin
289 transport (*MtPIN2–4*), rather than nodulation-specific pathways. This suggests that some of the
290 legacy traits identified in this study may be mediated through root growth and architecture,
291 which influence soil nutrient and water status and rhizosphere interactions, providing a
292 potential mechanistic link between mungbean genotype and subsequent wheat performance.

293 A trade-off was observed between mungbean yield and its legacy effects on wheat performance,
294 indicating that traits conferring high productivity in one crop may compromise the next crop
295 in rotation. Specifically, high-yielding mungbean genotypes were associated with reduced
296 wheat NDRE at flowering, which in turn was linked to lower wheat yield, consistent with a
297 source-sink limitation driven by environmental modification. This suggests that mungbean
298 genotypes may alter the soil environment through mechanisms such as differential nutrient
299 extraction, altered water availability, or rhizosphere-mediated shifts in the soil microbiome.
300 These changes may reduce resource availability for the subsequent crop, thereby impacting
301 biomass accumulation and final yield.

302 Genomic analysis revealed negative correlations between mungbean haplotype effects on
303 mungbean and wheat traits, with particularly strong trade-offs for yield. For instance,
304 haploblock b000055 showed that haplotypes associated with the highest mungbean yield also
305 had the most detrimental effect on legacy wheat yield, whereas b000942 included haplotypes
306 with neutral or even positive effects on both crops. Importantly, these 'correlation breakers'
307 occurred mostly in the lower effect size range, suggesting that system-level improvement may
308 be best achieved through genome-wide strategies like weighted genomic selection or haplotype
309 stacking, rather than marker-assisted selection for large-effect loci only.

310 Although the precise biological drivers of these legacy effects remain unclear, our targeted soil
311 analyses indicate that there is measurable variation in both nutrient availability and VOC
312 profiles among diverse mungbean genotypes (Supplementary Tables 5 and 7). While the
313 concept of microbes utilising VOCs for interkingdom communication is relatively recent
314 (Weisskopf, et al., 2021), soil volatilomic analysis holds promise as a cost-effective means to
315 assess soil health and microbial biodiversity. Several genotype-associated VOCs were
316 identified, including 2-pentylfuran, which is known to be emitted from crops roots and acts as

317 an insect attractant (la Forgia, et al., 2023), and 2-methylisoborneol and related terpenes, which
318 may indicate the presence of specific bacterial types such as actinobacteria, myxobacteria, and
319 cyanobacteria (Weisskopf et al., 2021; Martin-Sanchez, et al., 2019). While directly linking
320 these VOCs to specific microbes or plant processes requires additional investigation, these
321 findings highlight the potential for genotypic influence on the soil environment through root
322 architecture, nutrient and water acquisition, or microbial community structuring. In particular,
323 legacy effects mediated through persistent changes in the rhizosphere microbiome are a
324 promising avenue, as legume genotypes are known to establish distinct microbial communities
325 that can enhance nutrient cycling and disease suppression for subsequent crops (Yu et al., 2025;
326 Kirkegaard et al., 1997). Together, these findings underscore the need for further biological
327 characterisation of legacy mechanisms and demonstrate the feasibility of incorporating legacy
328 traits into breeding strategies to optimise productivity across crop rotations.

329 To evaluate the practical implications of these trade-offs, simulated genomic selection
330 strategies revealed clear consequences when breeding solely for single-crop performance
331 within a rotation system. When selection was fully weighted toward mungbean yield,
332 substantial genetic gain in mungbean (36.86%) was observed but consistent reductions in wheat
333 legacy yield (7.71%) were noted, reflecting negative genetic correlations between traits
334 expressed in the two crops. In contrast, selection indices designed to balance genetic gain in
335 both crops moderated these trade-offs (70:30 weighting) or eliminated them (50:50 weighting).
336 While absolute genetic gain in each crop was reduced, overall system performance improved
337 by minimising negative legacy effects. Most remarkably, equal weighting (50:50) achieved
338 simultaneous yield gains for both mungbean and wheat (19.45% and 7.55%, respectively),
339 demonstrating that direct and legacy traits under negative correlation can be successfully
340 managed through weighted selection indices. In practice, optimal weighting schemes could
341 consider economic factors including relative commodity prices, input costs such as nitrogen
342 fertiliser, and farm-specific production costs, as the economic value of legacy effects may vary
343 substantially depending on market conditions and production systems (Melton et al., 1979).
344 These simulations provide a framework for integrating legacy traits into breeding pipelines,
345 offering insights into how genomic prediction can be optimised to support multi-season, multi-
346 crop production.

347 The implications of breeding for legacy traits extend far beyond the immediate case study,
348 presenting a promising pathway to enhance agricultural sustainability by reducing input
349 dependency and improving system efficiency. By identifying legume genotypes that promote

350 beneficial downstream effects on cereals, breeders can select varieties that contribute residual
351 nitrogen, improve soil structure, modify soil microbiome, and maintain moisture availability,
352 thereby reducing resource inputs in subsequent crops. This approach can also extend beyond
353 sequential rotations to intercropping systems where genetic variation in root architecture,
354 nitrogen fixation efficiency, and rhizosphere interactions could enhance complementarity and
355 resource-use efficiency. The availability of modern genomic approaches now enable predictive
356 breeding decisions (Hayes et al., 2024) that could harness legacy effects for the first time, and
357 the ability to map these effects to defined genomic regions provides a foundation for
358 incorporating them into genomic prediction pipelines.

359 However, implementing this approach at scale requires a paradigm shift that aligns breeding
360 priorities across multiple crops or within large breeding programs that manage multiple crop
361 portfolios simultaneously. Current breeding programs and funding models are structured
362 around single-crop optimisation with economic incentives favouring direct trait improvements
363 over legacy effects. Transitioning to legacy trait breeding would require new collaborative
364 frameworks and revised intellectual property models that recognise contributions to farming
365 systems productivity, alongside logistically complex multi-location, multi-season trials to
366 validate genetic effect stability and build industry confidence. Legacy trait expression is likely
367 to exhibit significant genotype-by-environment interactions, particularly when soil properties
368 vary across target production environments, necessitating comprehensive testing to establish
369 breeding value stability. However, this investment in comprehensive testing will be essential
370 to build industry confidence and drive adoption of system-level breeding approaches.

371 As with any trait, studying and improving legacy effects requires sufficient genetic diversity.
372 Elite breeding materials may lack the variation necessary to detect and exploit these effects
373 compared to the mungbean diversity panel used in this research, necessitating the introgression
374 of required genetic variation into breeding populations. This case study also was conducted at
375 a single location with mungbean as the initial crop under nitrogen-deficient, rainfed conditions,
376 which does not fully capture the complexity of legacy dynamics in diverse commercial farming
377 systems. Nonetheless, yield from our mungbean mini-core experiments was similar to that of
378 previous research experiments under different management conditions and years
379 (Supplementary Fig 4). Furthermore, testing legacy effects across multiple wheat genetic
380 backgrounds would reveal whether these effects are consistent across cereal genotypes or if
381 specific legume-cereal genetic combinations maximise rotational benefits. Therefore, future
382 studies involving multi-location trials, diverse cropping systems, and multiple species with

appropriate genetic diversity are critical to explore the potential of this approach. Overall, this work provides the genetic and methodological foundation to enable breeding programs that optimise cropping systems rather than individual crops, offering a pathway for improved agricultural sustainability that harnesses genetic diversity to reduce external inputs while maintaining productivity.

Methods

Site preparation and nitrogen depletion

The experimental field site had characteristically high soil nitrogen levels typical of research stations due to fertiliser applications from previous trials. To create conditions more representative of commercial farming systems and conducive to evaluating genotypic variation in nitrogen fixation and legacy effects, soil nitrogen was deliberately depleted prior to sowing the mungbean panel. This was achieved by sequentially sowing grain sorghum and oat crops to maturity, which extracted residual soil nitrogen before being harvested and removed (Supplementary Fig 5). Soil sampling confirmed substantial nitrogen depletion before mungbean sowing (Supplementary Table 2), creating nitrogen-limiting conditions that would maximise expression of genotypic differences in nitrogen fixation capacity and enable quantification of legacy effects on the subsequent wheat crop.

Plant material and experimental design

A diverse mungbean panel of 309 genotypes was sown on 22nd January 2024 at the Department of Primary Industries research station in Gatton, Australia (27.55 °S; 152.33 °E) (Supplementary Fig 6). This panel included the mungbean mini-core collection, a diverse subset from the World Vegetable Center genebank representing 19 countries across Asia, Australia, Africa and the Americas (Schafleitner et al., 2015). An additional 25 mungbean genotypes and one black gram (*Vigna mungo*) cultivar was also included (Supplementary Table 8). The trial used an unbalanced replicated design with the mini-core collection replicated twice and the additional genotypes replicated four times. The experiment was designed using a model-based row-column design incorporating genetic relatedness using the R package 'od' (Cullis et al., 2020).

Mungbean genotypes were sown in 2-row 1.52 m × 4 m plots at a density of 25 plants m^{-2}. Mungbean seeds were inoculated with Group I inoculum (EasyRhiz™, New Edge Microbials Pty. Ltd) at sowing to promote nitrogen fixation through rhizobia establishment in root nodules. Granulock Starter Z fertiliser (Incitec Pivot Fertilisers) was applied as a basal application of 25

kg ha^{-1}. The mungbean trial was desiccated with glyphosate and machine harvested to determine grain yield when the check cultivar Crystal reached 90% black pod stage. All mungbean residue (shoot and stubble) was retained in situ, and no tillage was performed prior to wheat sowing, preserving the soil legacy conditions.

A single wheat cultivar (LongReach Raider) was sown 23 days after mungbean harvest (23rd May 2024) in the same paddock. Wheat plots (five-row, 1.52 m × 4 m) were positioned to exactly overlap with the previous mungbean plots, with a seeding rate of 120 plants m^{-2}. This spatial correspondence enabled traits measured in wheat to be directly mapped to the proceeding mungbean genotype. Upon maturity, wheat was machine harvested for grain yield determination.

Both trials were conducted under rainfed conditions with appropriate weed, insect and disease control implemented as required. Daily meteorological data (minimum and maximum temperature, rainfall) were obtained from an onsite weather station (Supplementary Fig 7).

Data Collection

Agronomic and physiological traits, as well as soil properties, were measured prior to and during both trials, either across the entire experiment or on a subset of diverse genotypes (Supplementary Fig 8).

Soil water and nutrient analyses

Prior to the commencement of the mungbean field trial, soil samples were taken from five soil cores across the paddock which were split into two depths (0-20 and 20-40cm) (Supplementary Table 9). Each sample was divided into two samples, the first was weighed, dried in 105°C oven, and then weighed again to calculate gravimetric water content (%). The second sample was used for analysis of extractable phosphorus (Colwell P), ammonium nitrogen (NH_4^+), and nitrate nitrogen (NO_3^-) using standard protocols described by Rayment and Lyons (2011). All analyses were performed by an accredited external laboratory using a SEAL AQ400 discrete analyser for colorimetric detection. All final concentrations were converted to mg/kg dry soil for reporting.

Colwell P was extracted using a 0.5 M sodium bicarbonate solution at a 1:50 soil-to-solution ratio. Samples were shaken for 16 hours, centrifuged, and filtered. Phosphorus concentrations in the extracts were determined colorimetrically using the ammonium molybdate–ascorbic acid

445 method, with potassium antimonyl tartrate added to control the reaction rate. Concentrations
446 measured in mg/L were converted to mg/kg based on extraction volume and soil mass.

447 Ammonium nitrogen (NH_4^+) was extracted using a 2 M potassium chloride (KCl) solution at a
448 1:10 soil-to-solution ratio and mixed for 1 hour. The resulting extracts were centrifuged and
449 filtered before analysis. Ammonium was quantified colorimetrically through its reaction with
450 sodium salicylate and nitroprusside in a mildly alkaline buffer, forming a coloured complex in
451 the presence of chlorine and detected at 650 nm.

452 Nitrate nitrogen (NO_3^-) was extracted following the same procedure as ammonium using 2 M
453 KCl. Nitrate was reduced to nitrite via a cadmium reduction column, and the resulting nitrite
454 was measured colorimetrically using a reaction with sulfanilamide and NED, with absorbance
455 read at 540 nm.

456 Additional soil nutrient analyses were undertaken prior to mungbean harvest from two
457 replicates of 10 diverse mungbean genotypes (AGG324187 (2B), AusTRC 324159, Berken,
458 Celera II-AU, CHIH-CO, CPI62672, Crystal, M10403, M10452 and Moong; Supplementary
459 Fig 9). In addition to P, NH_4^+ and NO_3^- being captured, exchangeable bases (Ca, K, Mg, Na)
460 were also measured by using a 1 M ammonium chloride solution at a 1:10 soil-to-solution ratio,
461 shaken for 1 hour. The extracts were centrifuged, filtered, and analysed using a Thermo iCAP
462 PRO XP ICP-OES instrument. Concentrations (mg/L) were converted to mg/kg using
463 extraction volume and soil mass. These values were further converted to milliequivalents
464 (meq/100g) by dividing the mg/kg concentration by the atomic weight of each ion, and then
465 adjusting for charge: divided by 10 for monovalent ions (Na^+, K^+) and by 5 for divalent ions
466 (Ca^{2+}, Mg^{2+}). Cation exchange capacity (CEC) was estimated from the sum of these
467 exchangeable cations.

468 *Soil microbiome analyses*

469 To investigate potential soil microbiome differences attributable to mungbean genotype, we
470 analysed soil volatile organic compounds (VOCs) as chemical indicators of microbial activity
471 and community composition. Soil samples were collected from the ten diverse genotypes
472 described above, and VOC profiles were characterised using headspace solid-phase
473 microextraction gas chromatography-mass spectrometry (HS-SPME-GC/MS).

474 The HS-SPME-GC/MS methodology was adapted from Rivers et al. (2019) for volatilomic
475 analysis of soil samples. Analysis was performed using an Orbitrap Exploris GC 240 Mass

476 Spectrometer fitted with a TriPlus RSH Multipurpose (i.e. Liquid and Headspace Injection,
477 SPME Arrow, and ITEX-DHS) Extended Rail (Thermo Fisher Scientific, Massachusetts,
478 USA). Splitless mode was employed for application of the VOCs via a 1.0 mm straight no-
479 wool liner to a TRACE 1610 series Gas Chromatograph (Thermo Fisher Scientific). Soil
480 samples, QC samples, laboratory blanks, and standards were block randomised throughout
481 each batch. Each sample was placed on 2 ml of 20% NaCl solution and incubated at 80 ˚C for
482 40 minutes with continuous agitation at 500 rpm to enhance VOC volatilisation and
483 homogenisation. VOC extraction (adsorption) was carried out by exposing a broad specificity
484 SPME Arrow fibre (1.10mm DVB/C-WR/PDMS 110µm x 20mm, Thermo Fisher Scientific)
485 to soil sample head space for 40 minutes with continuous agitation at 1000 rpm. Extracted
486 VOCs underwent desorption from the SPME Arrow on to the GC column (TraceGOLD TG-
487 5SilMS GC Column, Thermo Fisher Scientific) via the inlet at 250 ˚C for 10 minutes. Between
488 samples, the SPME Arrow fibre undergoes a pre- and post-conditioning at 250 ˚C for an
489 additional 10 minutes to prevent cross sample contamination. Chromatographic separation of
490 the soil VOCs was achieved employing ultra-pure helium as a carrier gas and via a 38.5 minutes
491 oven temperature program: 40 ˚C for 2 minutes , increasing to 150 ˚C at a ramp rate of 5 ˚C/min
492 and held for 2 minutes , then increased to 320 ˚C at 15 ˚C/min and held for 1 minute. Lastly,
493 the Orbitrap Exploris 240 MS was operated in full MS scan acquisition using electron
494 ionisation at 70eV from m/z 40-500 with a lag time of 5 minutes, and a Orbitrap resolution of
495 60,000. Temperatures were 320 ˚C for the auxiliary transfer line and 250 ˚C for the ion source.

496 Volatile data were processed using Thermo Compound Discoverer (ver. 3.3.2.31) for
497 deconvolution and data analysis. The NIST/EPA/NIH Mass spectral libraries (ver. 2023) were
498 used for mass spectral matching and peak annotations. Kovats non-isothermal retention indices
499 (RIs) were calculated using an *n*-alkanes (C7-C40) standard mix and compared to reference
500 semi-standard non-polar RIs from the NIST and PubChem databases when available. Peak
501 intensity values were collected and corrected based on the internal standard nitrobenzene,
502 background peak detection in blank samples, and sample weight. Subsequent statistical
503 analyses were carried out using MetaboAnalyst 6.0 (www.metaboanalyst.ca).

504 *Total aboveground biomass*

505 In the mungbean trial, biomass samples were harvested from 1-4 replications of a subset of 47
506 diverse lines. Sampling occurred when the commercial check cultivar Crystal reached
507 flowering (50% of the plot had open flower), which represented mid canopy development.
508 Samples were taken from 0.5 x 1.52 m of the two rows per plot. For the wheat trial, biomass

cuts were taken from the same plots as the preceding mungbean trial at heading. Samples were harvested from 0.5 x 0.75 m of the two middle rows per plot and dried at 65 ˚C for 5 days before weighing total biomass.

Vegetation indices

Vegetation indices were extracted from multispectral UAV imagery collected when mungbean check cultivar Crystal reached flowering and 90% black pod growth stages. Imagery collection and processing followed methods detailed in Van Haeften et al. (2025). Briefly, a MicaSense Altum™ sensor mounted on a Matrice 300 RTK UAV platform captured images that were processed into georeferenced orthomosaics using Pix4D software. Plot boundaries were defined in ArcMap for the mungbean trial and applied to the wheat trial to ensure corresponding wheat plots aligned with previous mungbean genotype plots. Normalized difference red edge index (NDRE), height, thermal and canopy coverage were extracted and used to estimate mungbean biomass at mid-canopy development (determined when Crystal had reached 50% flowering). Raw NDRE values were also extracted at 90% black pod stage in mungbean and at flowering in wheat.

Grain quality characteristics

To assess legacy effects on wheat quality in addition to yield, grain protein content was measured. Wheat grain protein content was determined using near-infrared spectroscopy with an Inframatic 9500 (IM9500) Grain Analyser (Perten Instruments). The instrument warmed up for a minimum of 30 minutes and self-calibrated using the internal reference standard per manufacturer recommendations. Approximately 200 g sub-samples were loaded into the IM9500 sample hopper for analysis. The IM9500 conducted three sub-sample readings and averaged spectra before predicting constituent values. Each sample was analysed in triplicate; between replicates, the hopper was emptied and refilled with fresh sample portions. Protein content was reported on a 12% moisture basis.

Statistical Analyses

Mungbean biomass prediction models

Mungbean biomass predictions used the UAV flight corresponding to mid-canopy development and ground-based biomass measurements collected on the same day. A prediction model previously developed for this growth stage (Van Haeften et al., 2025) was applied, incorporating height, thermal, NDRE, and coverage in a stepwise regression framework. Model validation used an 80/20 training/testing split.

541 ***Single-site spatial analyses***

542 Single site spatial analysis accounted for spatial variation across the site for all traits in both
543 crops. Both fixed and random row and column terms were tested for model improvement and
544 retained as needed. Wald statistics determined significance of fixed effects, while AIC, BIC
545 and log-likelihood assessed model fit changes due to added random components. Best Linear
546 Unbiased Estimators (BLUEs) and Best Linear Unbiased Predictors (BLUPs) were calculated
547 using equation 1:

548 $$y = Xb + Zu + e \quad (1)$$

549 where b is a vector of fixed effects, u is a vector of random effects, X and Z are the associated
550 design matrices and e is the residual.

551 Generalised broad sense heritability for each trait was calculated following Cullis et al (2006)
552 using equation 2:

553 $$H_g^2 = 1 - \frac{A_{tt}}{(2\gamma_v)} \quad (2)$$

554 where A_{tt} is the average prediction error variance and γ_v is the genetic variance estimated by
555 the model.

556 ***Correlations***

557 Phenotypic correlations between traits were calculated using Pearson's correlation coefficient
558 based on BLUEs for each genotype. Statistical significance was assessed using two-tailed p-
559 values, with non-significant correlations ($p > 0.05$) flagged in visualisations. The same
560 methodology was used to calculate correlations between haplotype variances and haplotype
561 effects.

562 Genetic correlations were calculated for each trait pair using mixed linear models with
563 unstructured variance structures applied to trait-to-trait interaction terms as per equation 3:

564 $$\begin{bmatrix} y_1 \\ y_2 \end{bmatrix} = \begin{bmatrix} X_1 & 0 \\ 0 & X_2 \end{bmatrix} \begin{bmatrix} \beta_1 \\ \beta_2 \end{bmatrix} + \begin{bmatrix} Z_1 & 0 \\ 0 & Z_2 \end{bmatrix} \begin{bmatrix} u_1 \\ u_2 \end{bmatrix} + \begin{bmatrix} \varepsilon_1 \\ \varepsilon_2 \end{bmatrix} \quad (3)$$

565 where y represents phenotype vectors for traits 1 and 2 respectively, X and Z are design
566 matrices for the fixed and random components of the model, β represents coefficient of fixed
567 effects, u represents the random genetic effects, and ε is the residual. Covariance between
568 genetic effects is represented as $Var(u) = G \otimes K$, where K is the genomic relationship matrix
569 (GRM) and G is the genetic covariance matrix between traits.

570 ***Genomic analyses***

571 To identify genomic regions underlying both direct mungbean performance and legacy effects
572 on wheat, haplotype-based mapping was conducted using the local genomic estimated breeding
573 value (local GEBV) method (Voss-Fels et al., 2019; Shaffer et al., 2025). DArTseq markers
574 were curated based on a minor allele frequency greater than 0.05, heterozygosity of less than
575 0.2, and <20% missing calls, resulting in 5,516 high-quality markers. Linkage disequilibrium
576 (LD) was explored to identify suitable thresholds for haploblock definition. The R package
577 'Selection Tools' defined haploblocks with markers in LD >0.3 and a marker tolerance of 4.
578 Marker tolerance represents the maximum number of markers that can be skipped during
579 haploblock creation, chosen based on the potential for misalignment. This approach defined
580 1,126 haploblocks with an average of 4.9 markers per block.

581 Marker effects were calculated using ridge-regression BLUP to determine simultaneous effects
582 of all SNPs per equation 4.

583 $$y = WGu + \varepsilon \quad (4)$$

584 where u is a vector of marker effects, G is the genotype matrix, W is a design matrix relating
585 genotypes to observations (y), and ε is the error. Relevant SNP effects were summed to
586 calculate haplotype effects at each haploblock. Effect variance was calculated for each
587 haploblock. For each trait, the top 1% of haploblocks by variance (12 haploblocks) were
588 identified as the most important.

589 ***Identifying and co-locating mungbean orthologues for functional legume genes***

590 Minimap2 (Li, 2018) was used to extract regions within high variance haploblocks based on
591 the Crystal reference genome enhanced with additional PacBio HiFi long-read sequencing data
592 (C. Mens & M. Udvardi, unpublished data). Mungbean orthologues of known nodulation and
593 nitrogen fixation genes were identified using reciprocal tBLASTn searches (E-value threshold
594 ≤ 1e-5) against a compiled list of over 200 characterised genes in model legume systems (Roy
595 et al., 2022). Orthologues were retained if overlapping with at least one of five key haploblocks
596 selected for their high variance for wheat yield and/or protein content.

597 ***Weighted selection strategies simulations***

598 Three breeding program scenarios were simulated to evaluate genetic improvement strategies:
599 1) selection for mungbean yield alone, 2) selection for legacy wheat yield alone, and 3)
600 simultaneous improvement of both crops. For the simultaneous improvement scenario,
601 selection used trait indices calculated as weighted sums of breeding values with

mungbean:wheat weightings of 0.7:0.3, 0.5:0.5, and 0.3:0.7. Simulations used SNP effects estimated from genomic prediction models to calculate genomic estimated breeding values (GEBVs). Each program ran 25 cycles, selecting 30 parents per cycle based on program-specific criteria. Selected parents were randomly mated to create 50 crosses, with 100 progeny per cross, generating 5,000 selection candidates for the next cycle. Genetic improvement was assessed by population mean GEBV changes per cycle. Each program was simulated five times, reporting average values and 95% confidence intervals of population mean GEBVs using the genomicSimulation R package (Villiers et al., 2022).

Comparison of genotypic differences for soil characteristics

To evaluate whether soil characteristics differed significantly among the subset of 10 diverse mungbean genotypes described in the soil nutrient analyses section, one-way analysis of variance (ANOVA) was performed for each measured soil variable. Genotype was treated as a fixed effect, and significance was assessed to determine whether plant genetic variation contributed to differences in soil nutrient concentrations and moisture content.

Acknowledgments

We thank the World Vegetable Center (WorldVeg), particularly Roland Schafleitner and Ram Nair, for providing the genomic data for the mungbean mini-core collection that formed the foundation of this study. We are grateful to the Queensland Department of Primary Industries for Gatton field trial support and provision of the Hermitage 2018 yield datasets. We particularly acknowledge the technical staff at the Gatton Research Facility for their assistance with field operations, and trial management. We thank LongReach Plant Breeders for generating the wheat grain protein data.

Data availability

All primary data supporting the findings of this study are available via The University of Queensland eSpace repository at https://doi.org/10.48610/cee8b66.

Funding

This work was supported by The University of Queensland start-up funds awarded to MS. Mungbean research conducted by MS, LH, MU at The University of Queensland was supported by the Australian Centre for International Agricultural Research International Mungbean Improvement Network Phase 2 (CIM2014/079) and Grains Research & Development Corporation Genetic Initiative to Transform Symbiotic Nitrogen Fixation in Australian Pulse Crops (UOQ2403-012RTX). LH was supported through an ARC Future Fellowship

(FT220100350). ED was supported by the Queensland Government's Industry Research Fellowships program (AQIRF096-2023RD6). SVH, ME were recipients of Grains Research & Development Corporation Research Scholarships (UOQ2101-003RSX; UOQ2410-011RSX). SVH, SMB were recipients of an Australian Government Research Training Program Scholarship. SMB was supported as a PhD student by the Deutsche Forschungsgemeinschaft (DFG) and University of Queensland International Research Training Group 2843 – Accelerating Crop Genetic Gain. ME was supported as a PhD student of the Australian Research Council Training Centre in Predictive Breeding for Agricultural Futures (IC230100016).

Authors contributions

Shanice Van Haeften: Writing – Original Draft Preparation, Investigation, Data Curation, Formal analyses, Visualisation. **Stephanie M. Brunner:** Writing – Original Draft Preparation, Data Curation, Formal analyses, Visualisation. **Eric Dingalsan:** Methodology, Writing – Review & Editing. **Edward Fabreag:** Formal analyses, Writing – Review & Editing. **Joseph Eyre:** Methodology, Investigation, Writing – Review & Editing. **Celine Mens:** Investigation**.** **Ben J. Hayes:** Supervision, Writing – Review & Editing. **Michael Udvardi:** Supervision**,** Writing – Review & Editing. **Samir Alahmad:** Investigation. **Mitchell Eglinton:** Investigation, Writing – Review & Editing. **Ryan McQuinn:** Investigation, Formal analyses, Writing – Review & Editing. **Merril Ryan**: Resources, Writing – Review & Editing. **Sarah van der Meer:** Investigation. **Millicent R. Smith:** Conceptualisation, Funding Acquisition, Project Administration, Writing – Review & Editing. **Lee T. Hickey:** Conceptualisation , Project Administration, Writing – Review & Editing.

Competing interests

The authors declare no competing interests.

References

Bennett, A. J., Bending, G. D., Chandler, D., Hilton, S. & Mills, P. Meeting the demand for crop production: the challenge of yield decline in crops grown in short rotations. Biol. Rev. 87, 52–71 (2012).

Cernay, C., Makowski, D. & Pelzer, E. Preceding cultivation of grain legumes increases cereal yields under low nitrogen input conditions. Environ. Chem. Lett. 16, 631–636 (2018).

Ellouze, W. et al. Chickpea genotypes shape the soil microbiome and affect the establishment of the subsequent durum wheat crop in the semiarid North American Great Plains. Soil Biol. Biochem. 63, 129–141 (2013).

Evenson, R. E. & Gollin, D. Assessing the impact of the Green Revolution, 1960 to 2000. Science 300, 758–762 (2003).

Foyer, C. H., Nguyen, H. & Lam, H. M. Legumes—the art and science of environmentally sustainable agriculture. Plant Cell Environ. 42, 1–5 (2019).

Hayes, B. J. et al. Potential approaches to create ultimate genotypes in crops and livestock. Nat. Genet. 56, 2310–2317 (2024).

Hickey, L. T. et al. Breeding crops to feed 10 billion. Nat. Biotechnol. 37, 744–754 (2019).

Ilyas, N. et al. Contribution of nitrogen fixed by mung bean to the following wheat crop. Commun. Soil Sci. Plant Anal. 49, 148–158 (2018).

Kirkegaard, J. A., Hocking, P. J., Angus, J. F., Howe, G. N. & Gardner, P. A. Comparison of canola, Indian mustard and Linola in two contrasting environments. II. Break-crop and nitrogen effects on subsequent wheat crops. Field Crops Res. 52, 179–191 (1997).

La Forgia, D., Martin, C., Turlings, T. C. & Verheggen, F. 2-Pentylfuran: an aggregation attractant for wireworms. Arthropod-Plant Interact. 17, 465–472 (2023).

Lago-Olveira, S., Rebolledo-Leiva, R., Garofalo, P., Moreira, M. T. & González-García, S. Environmental and economic benefits of wheat and chickpea crop rotation in the Mediterranean region of Apulia (Italy). Sci. Total Environ. 896, 165124 (2023).

Li, J. et al. Diversifying crop rotation improves system robustness. Agron. Sustain. Dev. 39, 38 (2019).

Li, L., Awada, T., Shi, Y., Jin, V. L. & Kaiser, M. Global greenhouse gas emissions from agriculture: pathways to sustainable reductions. Glob. Change Biol. 31, e70015 (2025).

Lilley, J. M. & Kirkegaard, J. A. Farming system context drives the value of deep wheat roots in semi-arid environments. J. Exp. Bot. 67, 3665–3681 (2016).

Martín-Sánchez, L. et al. Phylogenomic analyses and distribution of terpene synthases among Streptomyces. Beilstein J. Org. Chem. 15, 1181–1193 (2019).

Melton, B. E., Heady, E. O. & Willham, R. L. Estimation of economic values for selection indices. Anim. Sci. 28, 279–286 (1979).

Rivers, J. Y., Truong, T. T., Pogson, B. J. & McQuinn, R. P. Volatile apocarotenoid discovery and quantification in Arabidopsis thaliana: optimized sensitive analysis via HS-SPME-GC/MS. Metabolomics 15, 79 (2019).

Rose, T. J., Damon, P. & Rengel, Z. Phosphorus-efficient faba bean (Vicia faba L.) genotypes enhance subsequent wheat crop growth in an acid and an alkaline soil. Crop Pasture Sci. 61, 1009–1016 (2010).

Salvagiotti, F., Biassoni, M. M., Magnano, L. & Bacigaluppo, S. Enhanced seed yield of full-season soybean when rotated with cereals and cover crops as compared to monoculture in a long-term experiment. Eur. J. Agron. 161, 127382 (2024).

Shaffer, W., Papin, V., Yadav, S., Voss-Fels, K. P., Hickey, L. T., Hayes, B. J. & Dinglasan, E. G. Local genomic estimates provide a powerful framework for haplotype discovery. bioRxiv 2025-08 (2025).

Somenahally, A. et al. Microbial communities in soil profile are more responsive to legacy effects of wheat-cover crop rotations than tillage systems. Soil Biol. Biochem. 123, 126–135 (2018).

Villiers, K., Dinglasan, E., Hayes, B. J. & Voss-Fels, K. P. genomicSimulation: fast R functions for stochastic simulation of breeding programs. G3 12, jkac216 (2022).

Voss-Fels, K. P., Cooper, M. & Hayes, B. J. Accelerating crop genetic gains with genomic selection. Theor. Appl. Genet. 132, 669–686 (2019).

Voss-Fels, K. P. et al. Breeding improves wheat productivity under contrasting agrochemical input levels. Nat. Plants 5, 706–714 (2019).

Weisskopf, L., Schulz, S. & Garbeva, P. Microbial volatile organic compounds in intra-kingdom and inter-kingdom interactions. Nat. Rev. Microbiol. 19, 391–404 (2021).

Yu, S., Wang, T., Wang, L., Yao, S. & Zhang, B. Preceding crop rotation systems shape the selection process of wheat root-associated bacterial communities. J. Integr. Agric. 24, 739–753 (2025).

Zhao, J. et al. Global systematic review with meta-analysis reveals yield advantage of legume-based rotations and its drivers. Nat. Commun. 13, 4926 (2022).